

Predicting End Bearing Capacity of Post-Grouted Drilled Shaft in Cohesionless Soils

Gray Mullins, M.ASCE¹; Danny Winters²; and Steven Dapp³

Abstract: Although pressure grouting beneath the tips of drilled shafts had been used successfully worldwide for close to 4 decades, it has remained relatively unused in the United States in part due to the absence of a rational design procedure. Previous international usage relied predominantly upon experience and unpublished proprietary approaches. More recently, research aimed at quantifying the improvement that could be derived from postgrouting drilled shaft tips has resulted in a design methodology. This paper briefly discusses the postgrouting process and outlines the full scale test programs used to identify parameters affecting postgrouting performance. Correlations developed between applied grout pressure and end bearing improvement are presented along with a numerical example illustrating the design procedure.

DOI: XXXX

CE Database subject headings: Drilled shafts; Bearing capacity; Cohesionless soils; Grouting; Design criteria; Predictions.

Introduction

The unit ultimate end bearing of drilled shafts tipped in cohesionless soil can be on the order of 20 times the unit ultimate side shear. However, this enormous capacity is rendered virtually unusable due to multiple mechanisms associated with construction techniques and soil mechanics. The two primary construction-related mechanisms that hamper end bearing development include: (1) soil relaxation beneath the shaft tip due to excavation and (2) debris remaining after cleanout. Furthermore, even under ideal shaft construction conditions, ultimate side shear is developed in only a fraction of the displacement required to develop the ultimate end bearing. The side shear fully develops at a displacement between 0.5 and 1.0% of the shaft diameter (D); whereas, the end bearing is fully mobilized at displacements of 10–15% D (Bruce 1986; Mullins et al. 2000). Therefore, the end bearing requires 10–30 times more displacement than side shear in order to mobilize the same percentage of its ultimate value. As a result, engineers typically must discount or significantly reduce the end bearing contribution to the capacity of drilled shafts to accommodate service/displacement limits.

In 1999, a 4 year study was initiated to quantify the effects of pressure grouting beneath the base of drilled shafts and show its

potential to mitigate the above mechanisms plaguing end bearing capacity. This method was expected to be applicable to projects with deep cohesionless deposits where the soil strata would require excessively long drilled shaft lengths without considerable end bearing contribution and in urban areas where vibrations associated with pile driving are not well tolerated. This paper briefly discusses the results from this study and introduces a new design procedure for predicting end bearing capacity in postgrouted drilled shafts tipped in cohesionless soils.

Background

In the early 1960s, efforts to improve the end bearing of drilled shafts began in Europe using high pressure grout injected beneath the shaft tip (Bolognesi and Moretto 1973; Gouvenot and Gabiax 1975; Sliwinski and Flemming 1984). Thereafter, numerous case studies have been documented stating its effectiveness. This end bearing modification technique, also called postgrouting or base grouting, has been used worldwide, yet literature on its use lacks a rational design approach. As a consequence, there has been little use in the United States. As this paper focuses on the design of the end bearing capacity, a thorough overview of postgrouting processes can be found elsewhere (Bruce 1986; Mullins et al. 2000).

In general, the postgrouting technique involves casting drilled shafts with a grout delivery system incorporated into the reinforcing cage capable of placing high pressure grout at the base of the shaft (after the shaft concrete has cured). This both densifies the in situ soils and compresses any debris left by the drilling process. Moreover, by preloading the soil beneath the tip, end bearing capacity can be developed within service/displacement limits. In previous studies, it was suggested that pressure-grouted shafts tipped in loose to medium dense sand provided the most benefit, but improvement was observed in all soil types cited. Specifically, end bearing could be improved in sands and clays with ultimate capacities as much as two to three times conventional ungrouted shafts (Bruce 1986). The same sources purported end bearing improvement to be dependent on the volume of grout injected.

¹Associate Professor, Dept. of Civil and Environmental Engineering, Univ. of South Florida, 4202 E. Fowler Ave., ENB 118, Tampa, FL 33620 (corresponding author). E-mail: gmullins@eng.usf.edu

²Research Associate, Dept. of Civil and Environmental Engineering, Univ. of South Florida, 4202 E. Fowler Ave., ENB 118, Tampa, FL 33620. E-mail: dwinters@eng.usf.edu

³Principal, Dan Brown & Associates, 300 Woodland Rd., Sequatchie, TN 37374. E-mail: sdapp@danbrownandassociates.com

Note. Discussion open until September 1, 2006. Separate discussions must be submitted for individual papers. To extend the closing date by one month, a written request must be filed with the ASCE Managing Editor. The manuscript for this paper was submitted for review and possible publication on March 16, 2005; approved on August 11, 2005. This paper is part of the *Journal of Geotechnical and Geoenvironmental Engineering*, Vol. 132, No. 4, April 1, 2006. ©ASCE, ISSN 1090-0241/2006/4-1-XXXX/\$25.00.

$$GP_{max} = 4q_s L/D \tag{3}$$

where GP_{max} =maximum predicted grout pressure; q_s =unit side shear; and L/D =shaft length to diameter ratio.

From a more practical perspective, several ranges are also identified in Fig. 2 that denote applicable limits on grout pressure. The lines denoting unit side shear values present upper bounds on grout pressure for shafts constructed in soils with average unit side shear values of 0.05, 0.1, and 0.2 MPa (0.5, 1.0, and 2.0 tsf). For all soils and L/D ratios, an upper limit on grout pressure is typically applied that considers the construction limitations of the grout pump, grout tubes, or the working life of the neat cement grout. Although pressures as high as 11 MPa (1,600 psi) are attainable, a 6.9 MPa (1,000 psi) upper limit is more realistic without having to use specialized equipment.

An example lower limit is also presented that represents the hydrostatic pressure of wet concrete for a 1 m diameter shaft. Assigning a grout pressure at or below this level does not provide a benefit worthy of the effort. Although in some instances the process of merely flushing grout through the tubes and grouting cell has shown grout volume taken into soft areas or unexpected voids, far more can be derived from a pressure grouting protocol that takes full benefit from an optimized design.

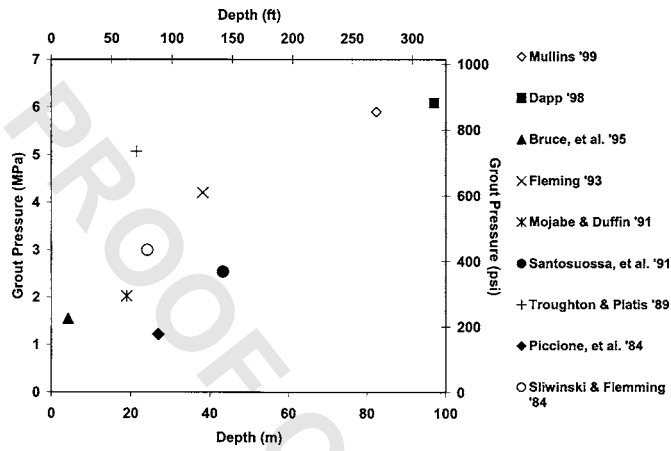


Fig. 1. Published grout pressure versus depth prior to this research program [Mullins (1999); Dapp (1998); Bruce et al. (1995); Fleming (1993); Mojabe and Duffin (1991); Santosuossa et al. (1991); Troughton and Platis (1989); Piccione et al. (1984); Sliwinski and Flemming (1984)]

However, the improvement was shown to be more directly related to grout pressure by the authors and forms the basis of the new design method.

During base grouting, the grout pressure produces a bidirectional force at the shaft tip, wherein the development of the end bearing is resisted by the skin friction of the shaft. Hence, longer shafts or shafts that develop more side shear can resist higher grout pressure. Previous studies that cited both the applied grout pressure and shaft length (or depth) show an increasing trend of grout pressure with depth (Fig. 1). This is in keeping with the understanding that the maximum grout pressure is dependent on the available side shear on which the grout pressure can react.

In concept, the anticipated grout pressure for a given site can be generalized with respect to the shaft length, diameter, and the average unit side shear (Fig. 2). As the grout pressure is a function of tip area, unit side shear, and shaft length, the expression for anticipated grout pressure can be simplified as follows:

$$GP_{max} = \text{side shear force}/\text{tip area} \tag{1}$$

$$GP_{max} = (q_s \pi DL)/(\pi D^2/4) \tag{2}$$

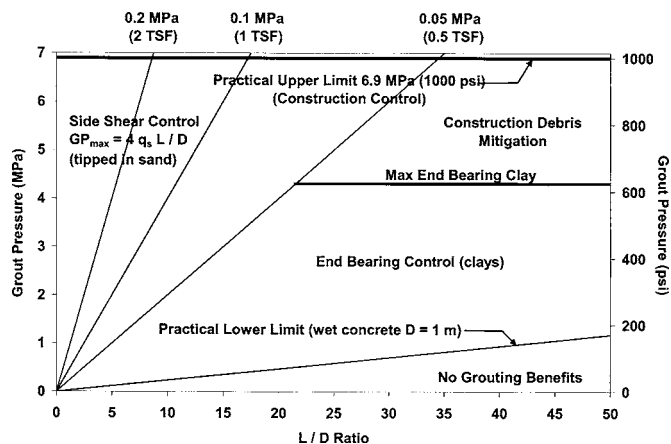


Fig. 2. Concept graph of pressure versus depth

End Bearing Development

Reese and O'Neill (1988) showed that the end bearing capacity of conventional ungrouted shafts could be expressed as a function of shaft diameter and the permissible settlement (Fig. 3). Therein, the ultimate design capacity based on 5% displacement was given by

$$q_b = 0.057N \tag{4}$$

where q_b =ultimate unit end bearing capacity (MPa); and N =uncorrected standard penetration test (SPT) blow count.

At displacements less than 5% D , a reduced capacity should be assigned using a tip capacity multiplier (TCM < 1) based on the above relationship and the permissible displacement; at larger dis-

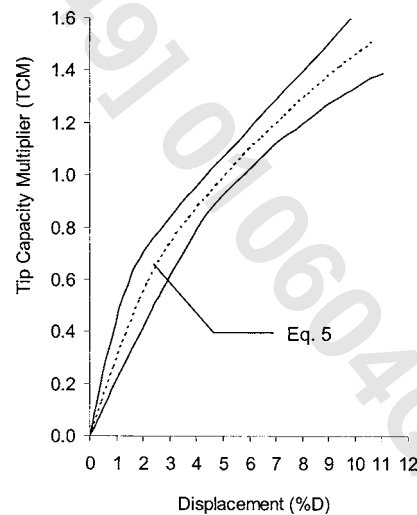


Fig. 3. Usable end bearing as function of permissible displacement (adapted from Reese and O'Neill 1988)

placements beyond 5% *D* even more end bearing can be developed ($TCM > 1$). Eq. (5) provides a convenient curve fit for the TCM trend shown in Fig. 3

$$TCM = \frac{\%D}{0.4(\%D) + 3.0} \quad (5)$$

TCM values greater than 1.0 corroborate Bruce's (1986) statement that shafts tipped in sand could continue to develop capacity up to 15% *D*. Unfortunately, large displacements such as these are rarely permissible due to service limits. For example, a 1.2 m (4 ft) diameter shaft would have to displace 61 mm (2.4 in.) in order to achieve ultimate capacity; whereas the side shear would develop in 6–12 mm (0.24–0.48 in.), shown in Fig. 4. At full side shear development, only about a third of the design end bearing has been developed. As an alternate, postgrouting beneath the shaft tip provides a method to avail higher usable end bearing at more reasonable displacements.

Effects of Side Shear Capacity on Grout Pressure

The grout pressure required to affect end bearing improvement in cohesionless soil is dependent on the available side shear. As such, uplift of the shaft is possible as the force from the applied grout pressure over the area of the toe approaches the ultimate side shear capacity. At this point, the grout pressure has both displaced/compressed the soil beneath the toe and strained the side shear in uplift. Depending on whether the grout pressure is maintained or released during the curing of the grout, two stress states may exist. Figs. 5 and 6 conceptually show the load history of the side shear and soil beneath the toe during the grouting and structural loading phases for maintained and released grout pressure, respectively. Four points are highlighted on each graph showing pertinent phases: Point (1), the initial unstressed state; Point (2), the maximum applied grout pressure; Point (3), the grout cured, prior to structural loading; and Point (4), after structural loading assuming a 1% *D* settlement. Although the mechanism by which the load is transferred into the soil is significantly different for the two approaches, the net effect is virtually identical with regards to load carrying capabilities.

When the grout pressure is maintained or locked-in during curing (Fig. 5), the toe load required to hold the shaft in negative

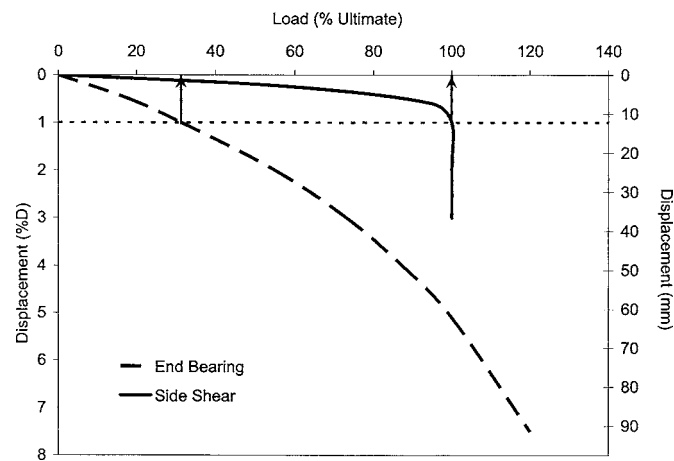


Fig. 4. Typical displacement mismatch between end bearing and side shear

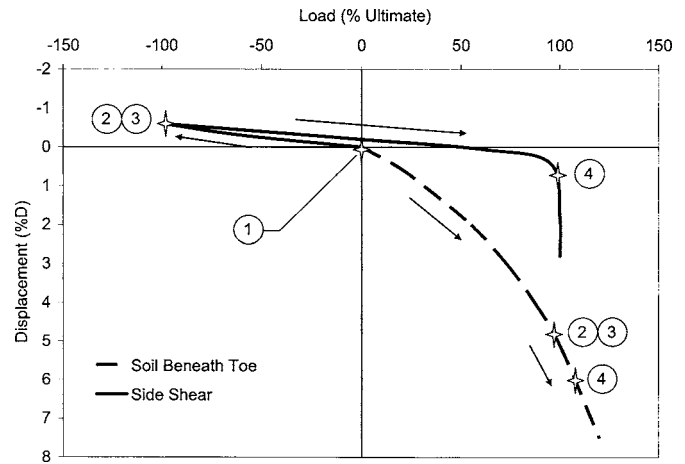


Fig. 5. Conceptual load/displacement history for locked-in grout pressure

side shear increases slightly as applied structural loads overcome the negative side shear (small displacements). In effect, the side shear load required to hold the soil beneath the toe in compression is replaced by the structural loading until the negative side shear is completely overcome, after which, additional load can be developed by positive side shear and a further increase in end bearing. The load carrying mechanism from precompressing the toe soils is analogous to pretensioning bolts used for tensile loading. Therein, bolts are commonly pretensioned during installation to over 90% of the usable capacity. This causes a clamping force that equals the sum of the bolt group pretensioning. The tensile loads in the bolts remain the same throughout the life of the connection but are ultimately resisted by a combination of structural loads and clamping forces. If the structural loads exceed the initial clamping force, plate separation occurs and the remaining 10% of the bolt capacity can be mobilized as needed up to the ultimate load. Fig. 7 shows the similarities between postgrouted shaft tips and a bolted tension connection (the bolt analogy is explained in italics).

When the grout pressure is released before curing or unlocked (Fig. 6), the soil beneath the toe is loaded normally during grouting, allowing large precompressing displacements to occur followed by a relatively stiff unloading. The side shear is stressed

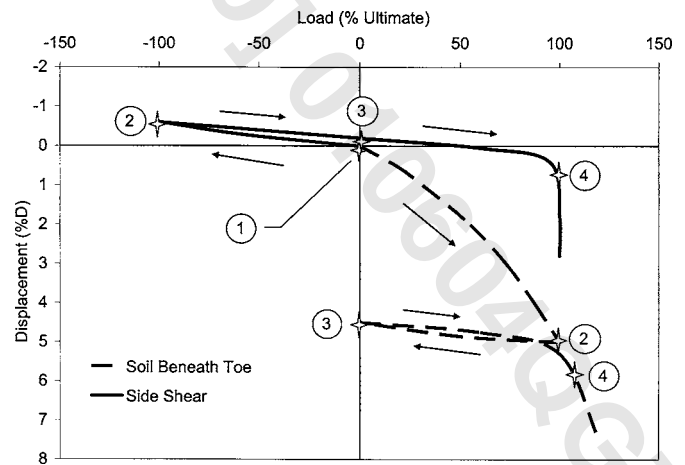


Fig. 6. Conceptual load/displacement history for unlocked grout pressure

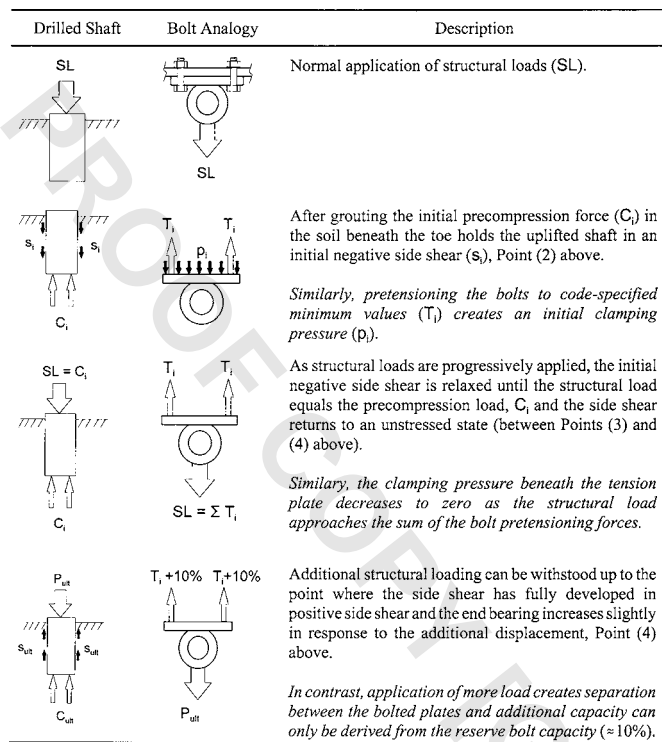


Fig. 7. Comparison of bolt pretensioning to shaft tip precompression

upward and returned to its unstressed state. Upon application of structural loading, the side shear develops normally (acting upward) while the end bearing is reloaded along a much stiffer path where the displacement required to fully develop the end bearing is commensurate with that of the side shear.

Minimal differences have been observed in the resultant capacity from these two mechanisms (Frederick 2001; Mullins and Winters 2004). In reality, some relaxation occurs in the soil beneath the toe even when the pressure is locked in. Consequently, the actual response in these cases reflects a combination of both scenarios.

The design method presented herein stems from a database of 26 grouted and ungrouted test shafts tipped in sand, silt, and clay at eight different sites which incorporated both locked-in and unlocked approaches. Five of these sites had shafts tipped in sand,

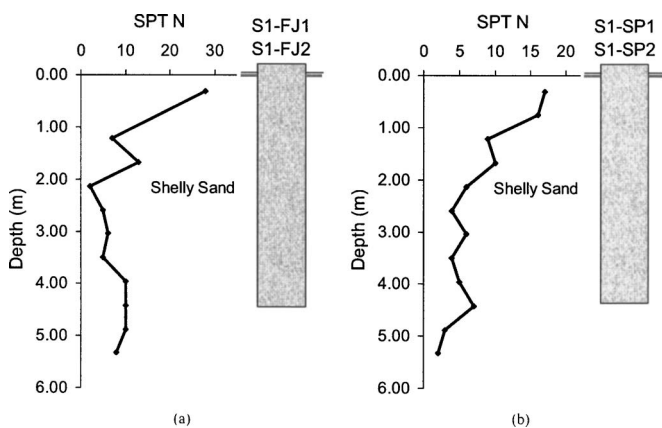


Fig. 8. Soil boring logs for site I (a) flat-jack and (b) sleeve-port test shafts

silty sand, shelly sand, or slightly cemented sand. This paper focuses on the improvement in cohesionless soils. Therefore, a discussion of the sites in cohesive soils is not presented within this paper.

Full-Scale Field Study

The research program consisted of both model-scale and full-scale testing. Model-scale testing was carried out within a frustum confining vessel and explored parameters affecting postgrouting performance and cavity expansion where the shafts could be easily exhumed (Frederick 2001; Mullins et al. 2001; Dapp 2002; Mullins and Winters 2004). The objective of the field studies were threefold: (1) to quantify the improvement that could be developed by pressure grouting the tip of the shaft; (2) to develop design recommendations for the use of pressure grouting drilled shaft tips; and (3) to establish criteria/guidelines for effective grouting. Although, the majority of sites included a control shaft (conventional, with no postgrouting), the response of the grouted shafts was also compared to end bearing design capacity predictions from soil boring logs (i.e., AASHTO 1999).

Two different grout distribution systems were used throughout the study: the flat jack and the sleeve port (also known as tube-a-manchette). Each system has associated advantages, but both provided similar end bearing improvement. A full discussion of these systems can be found elsewhere (Mullins et al. 2001; and Dapp 2002). The ensuing sections outline the site conditions and load test results for each of the sites where shafts were tipped in sandy soils.

Sites I and II: Clearwater, Fla.

A total of eight shafts were constructed and tested within two adjacent sites located in Clearwater, Fla. These shafts each had a diameter of 0.61 m (2.0 ft) and were 4.57 m (15 ft) in length. Five shafts, including one control shaft, were tested in Site I (loose to medium dense shelly sand); while three shafts, including one control shaft, were tested in Site II (loose silty sand). Soil exploration involved minicone (2.5 cm²) and full-size (10 cm²) cone penetration soundings as well as standard penetration testing. The minicone was used to quickly delineate site variability, the 10 cm² cone was used at each shaft location, and the SPT borings were conducted between the shaft locations. Excavation was conducted using polymer slurry for stabilization. Full details

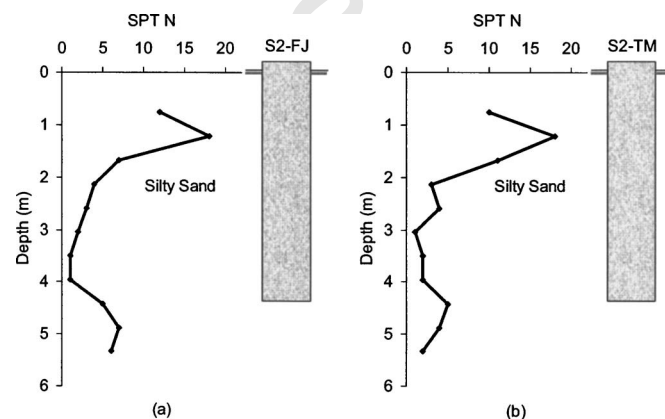


Fig. 9. Site II soil boring logs for test shafts (a) S2-FJ and (b) S2-TM

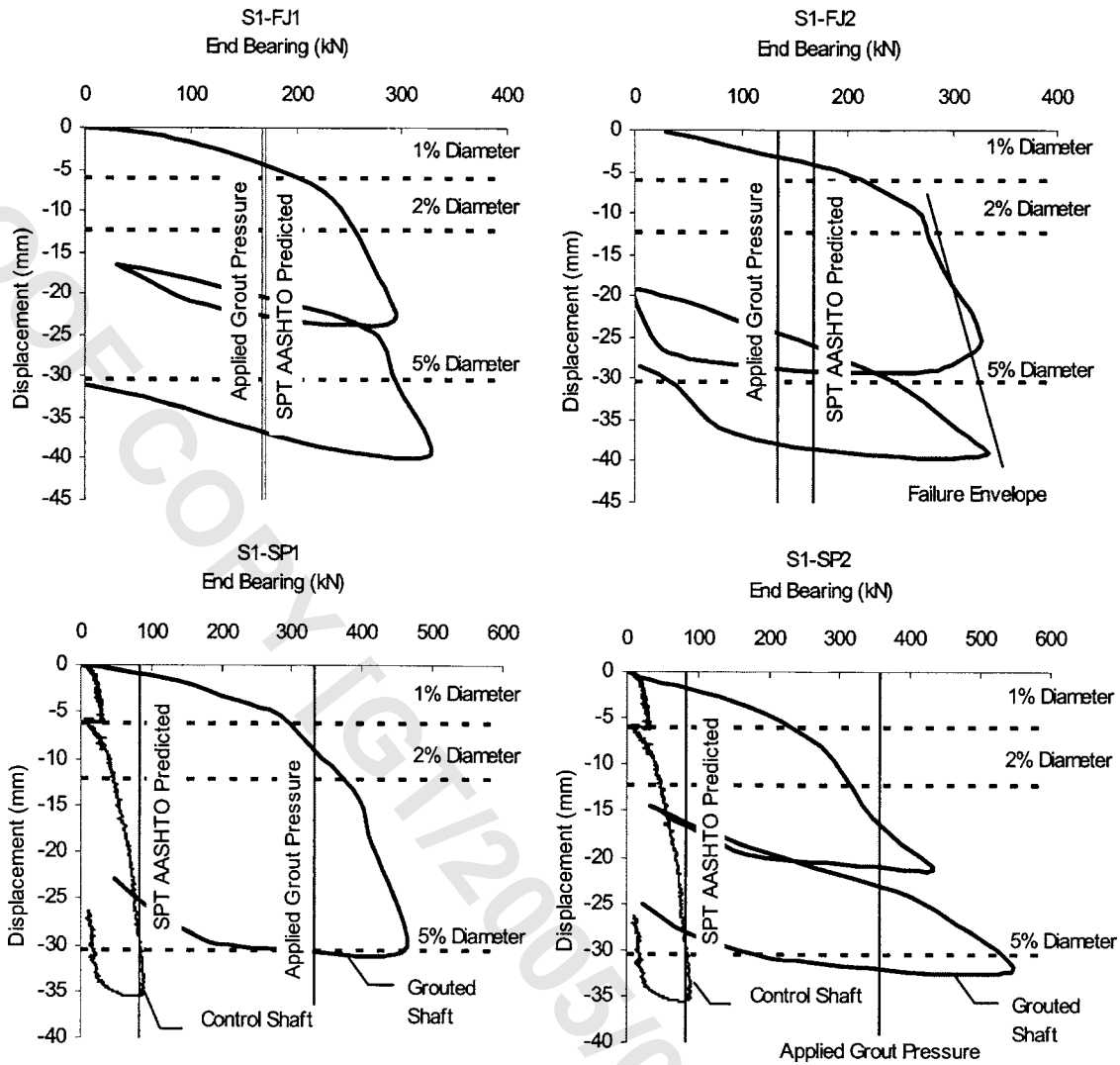


Fig. 10. Load test results for site I

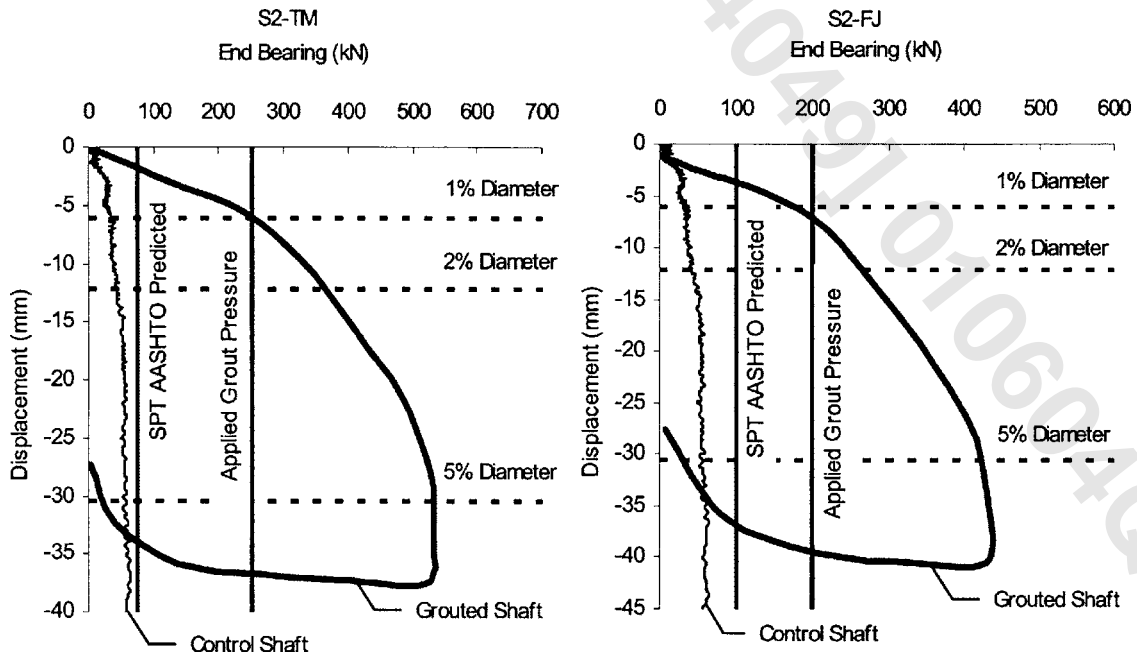


Fig. 11. Load test results for site II

Table 1. Full-Scale Field Study Results

Shaft I.D.	q_p Ultimate ^a (kPa)	Grouted capacity TCM			Applied grout pressure (kPa)	GPI
		1% <i>D</i>	2% <i>D</i>	5% <i>D</i>		
S1-FJ1	574	1.22	1.50	1.79	586	1.02
S1-FJ2	574	1.21	1.67	1.91	462	0.80
S1-SP1	287	3.48	4.44	5.51	1,138	3.96
S1-SP2	287	3.09	4.06	6.18	1,220	4.25
S2-FJ	344	1.69	2.58	4.18	683	1.98
S2-TM	258	3.33	4.72	7.09	862	3.34
S3-LT3	2,178	0.60	N/A ^b	N/A ^b	3,447	1.58
S4-LT2	630	3.15	4.40	5.84	5,240	4.68
S5-S2	3,969	1.05	1.30	1.63	1,157	0.69

^aReese and O'Neill (1988) [Eq. (4)].

^bUnable to fully mobilize test shaft during testing (see Fig. 12).

can be found elsewhere (Mullins et al. 2000; 2001; Dapp and Mullins 2002). Figs. 8 and 9 show the soil profiles for Sites I and II, respectively. Likewise, Figs. 10 and 11 show the load-displacement responses for each test shaft for the two sites as well as the applied grout pressure load and AASHTO predicted end bearing values. In each graph the capacities at displacements of 1, 2, and 5% *D* are indicated for future reference (also provided in Table 1).

Site III: Palm Beach, Fla.

Three test shafts, grouted and ungrouted, were constructed and tested in slightly cemented coquina sand located at the Royal Park Bridge crossing the Intracoastal waterway in Palm Beach, Fla. One of these shafts, LT-3, is a 1.22 m (4.0 ft) diameter, 34.80 m (114.2 ft) long grouted shaft. A combination of temporary and permanent casing was used with a sea water drill slurry. Fig. 12

shows the SPT soil boring and the end bearing results for LT-3. Additional information for Site III can be found in Dapp and Mullins (2002).

Site IV: West Palm Beach, Fla.

Two test shafts, grouted and ungrouted, were constructed and load tested as part of the PGA Blvd Grade Separation Bridge Project in West Palm Beach, Fla. The load test program for this site revolved around the relative end bearing performance of two 0.91 m (3 ft) diameter, 18.3 m (60 ft) long test shafts constructed in loose to medium dense shelly sand. Test shaft LT-1 served as the ungrouted control while LT-2 was grouted. Each shaft was constructed with a mineral slurry. A SPT boring was performed at the centerline of each test shaft. The SPT soil boring and end bearing results for LT-2 are shown in Fig. 13.

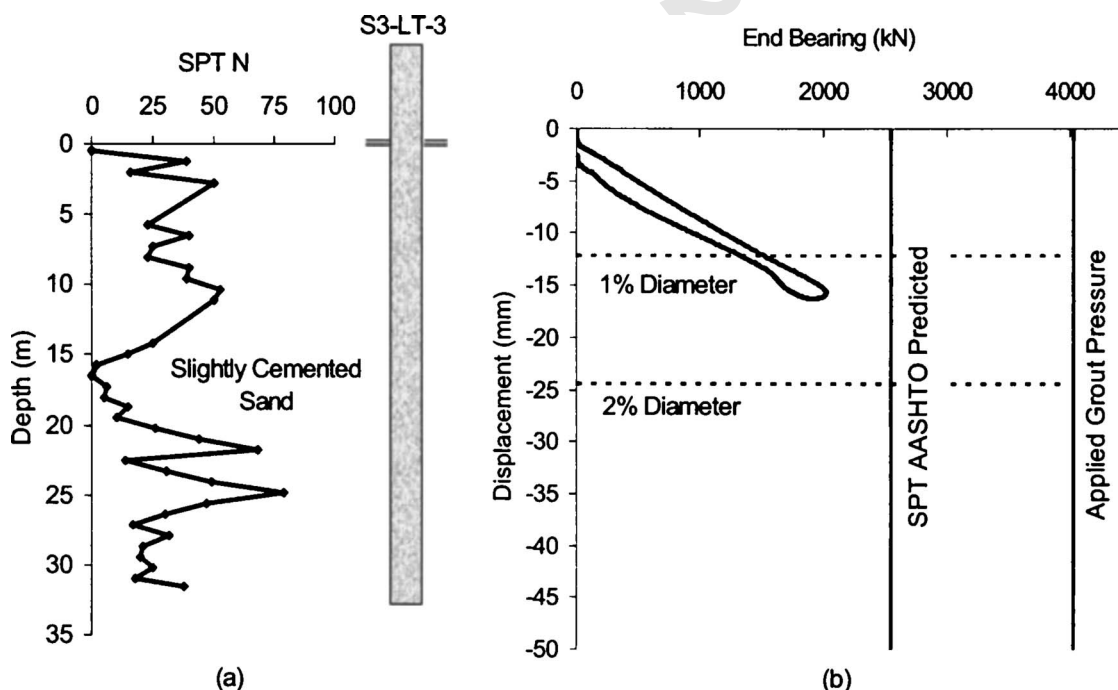


Fig. 12. Site III (a) soil boring log and (b) end bearing load test results for test shaft LT-3

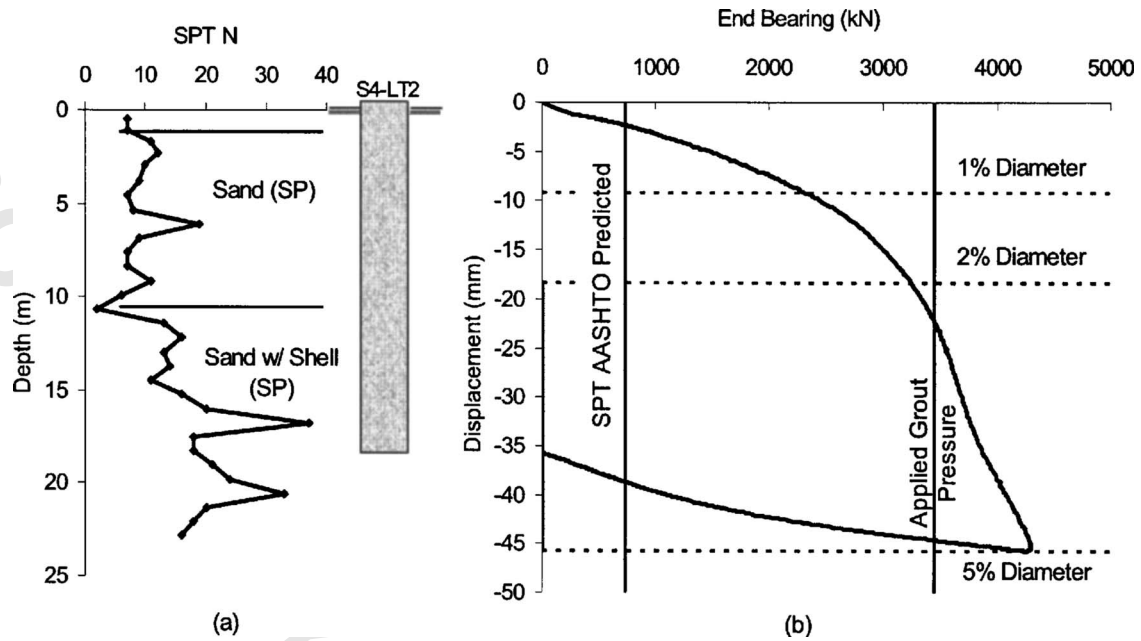


Fig. 13. Site IV (a) soil boring log and (b) end bearing load test results for test shaft LT-2

Site V: Houston, Tex.

Testing at Site V (dense sand) was a collaboration between the Univ. of Houston (UH) and the Univ. of South Florida (USF) to demonstrate to the Texas Department of Transportation the effectiveness of post grouting drilled shafts in soils native to the Houston region. A total of four 1.22 m (4.0 ft) diameter drilled shafts were constructed. A target load of 17.8 MN (2,000 t) was used in determining the shaft lengths. Two shafts were tipped in sandy soil while the other two shafts were tipped in clayey soil. Each pair of test shafts included a control shaft and a grouted shaft. The subsurface investigation of the test site was performed using three primary methods of exploration: standard penetration tests (SPT);

Texas cone penetration tests (TCP); and cone penetration tests (CPT). All shafts were constructed using mineral slurry. Fig. 14 shows the SPT soil boring and load test results for test shaft S-2 (tipped in sand and grouted). A full geological and load test discussion for this site can be found in Mullins and O’Neill (2003).

End Bearing Results

Many design methodologies exist for the calculation of drilled shaft tip capacities in sandy soils. For example, AASHTO (1999) presents four methods from which this determination can be made. These methods vary in the required parameters but use

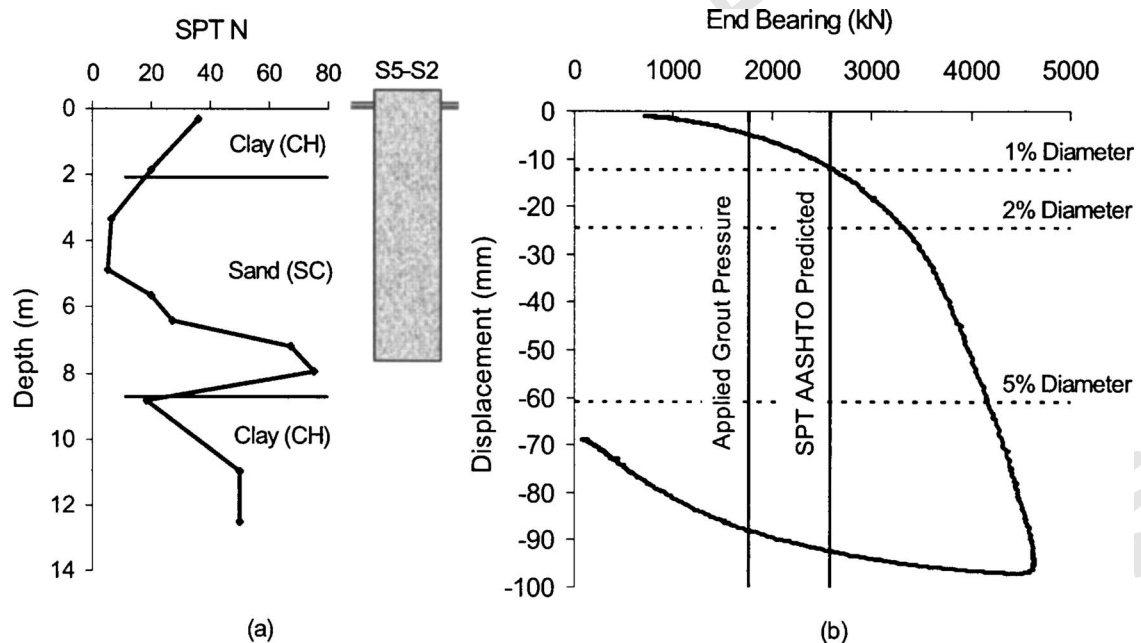


Fig. 14. Site V (a) soil boring log and (b) end bearing load test results for test shaft S-2

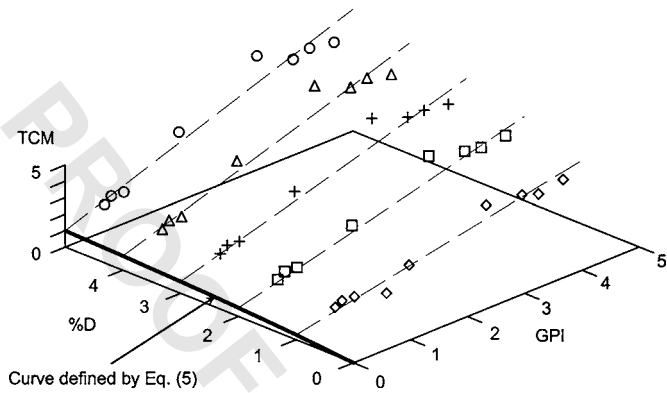


Fig. 15. Full-scale field study results

either SPT N values, the relative density state, and/or the depth of embedment expressed as a multiple of the diameter to calculate the end bearing capacity. An important aspect of this capacity determination is the displacement at which the capacity will be developed. Some methods clearly state this criterion as a percentage of the shaft diameter or as some service limit displacement (e.g., 5% of D , or 1 in.), while other methods do not.

This research project used the Reese and O’Neill (1988) method [Eq. (4)] to predict the ultimate end bearing capacity from SPT values as well as load test data. Table 1 provides details from each of the full-scale grouted test shafts expressed as a multiple of the Reese and O’Neill predicted capacity. The end bearing improvement is given in terms of the tip capacity multiplier (TCM), for the measured end bearing at 1, 2, and 5% D displacements. As the end bearing improvement is dependent on the applied grout pressure, the grout pressure is also listed both dimensionally (in kilo Pascal) and nondimensionally [as the grout pressure index (GPI)]. The GPI is defined as a nondimensional ratio of the applied grout pressure to the ungrouted end bearing at a displacement of 5% D [Eq. (4)]. The applied grout pressure was taken as the maximum sustained grout pressure and not a short duration pressure spike.

Design of Postgrouted Tip Capacity

To quantify the improvement with respect to standard design practice, a predictive approach was established on the basis of the

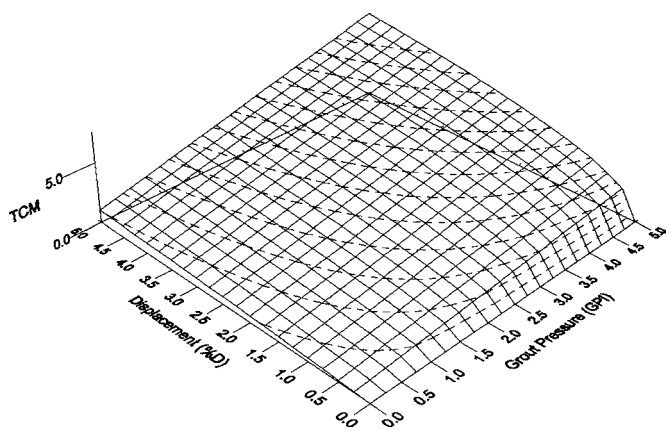


Fig. 16. Surface defined by TCMs derived from load test data dependent on grout pressure and displacement

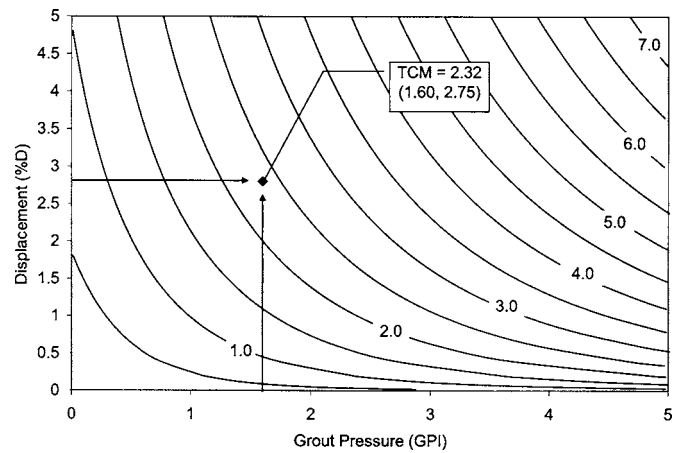


Fig. 17. TCM contours easily adapted for design applications

TCM and the GPI. The TCM was defined as a function of displacement and grout pressure. By plotting the results from Table 1 (Fig. 15), a surface can be defined that incorporates both the effects of grout pressure and permissible displacement (Fig. 16). Dashed lines in Fig. 16 show lines of constant TCM while solid lines show lines of constant displacement and grout pressure.

The plane defined by the displacement and TCM axes intersects the surface forming a hyperbolic relationship identical to the centerline trend that Reese and O’Neill published in 1988 shown in Figs. 3 and 15. Therein, when the GPI=0 no improvement is expected and it therefore predicts the same capacity as an ungrouted shaft. Likewise, when the permissible displacement approaches zero, so does the predicted mobilized capacity. A more usable form of this surface is given in Fig. 17 which shows the TCM contours. Given the GPI and displacement, the TCM can be estimated using Fig. 17 or with the following empirical relationship:

$$TCM = 0.713(GPI)(\%D)^{0.364} + \frac{\%D}{0.4(\%D) + 3.0} \quad (6)$$

The surface defined by Fig. 16 is nonlinear with respect to $\%D$ but linear with respect to variations in GPI. As the GPI and the TCM are both ratios based on the ungrouted end bearing, both the TCM and GPI increase or decrease similarly dependent on the ungrouted end bearing selected. Therefore, the TCM is only mildly affected by the method of determining the ungrouted end bearing. At high GPI values and low $\%D$ values, the TCM is insensitive to the ungrouted prediction method. As GPI approaches zero, the grouted end bearing approaches the ungrouted capacity and therefore is subject to the conservatism or unconservatism associated with whatever method was used to estimate the ungrouted capacity.

Design Procedure

For a given shaft diameter and embedment length, the method for estimating the unit end bearing of grouted shafts involves the following steps:

1. Calculate the ungrouted end bearing capacity at 5% D displacement, q_p Ultimate.
2. Calculate the ultimate side shear resistance, F_s , for the total length of embedded shaft.

3. Divide the ultimate side shear resistance by the cross-sectional area, A , of the shaft to determine the maximum anticipated grout pressure, GP_{\max}

$$GP_{\max} = \frac{F_s}{A} \quad (7)$$

4. Calculate the GPI as the ratio of the maximum anticipated grout pressure (Step 3) to the ungrouted unit tip resistance (Step 1)

$$GPI = \frac{GP_{\max}}{q_{p_Ultimate}} \quad (8)$$

5. Establish the maximum permissible service displacement as a ratio of the shaft diameter, $\%D$.
6. Determine the tip capacity multiplier given the grout pressure index (Step 4) and the permissible displacement (Step 5) using Fig. 17 or Eq. (6).
7. Estimate the grouted unit tip resistance as the product of the tip capacity multiplier (Step 6) and the ultimate ungrouted end bearing capacity (Step 1)

$$q_{\text{grouted}} = (TCM)(q_{p_Ultimate}) \quad (9)$$

For example, a 0.91 m (3 ft) diameter drilled shaft with an ultimate side shear resistance of 1,780 kN (200 t) will have a grouted end bearing capacity of 3.97 MPa (41.8 tsf). This is with a permissible shaft displacement of 25 mm (1 in.) and an ungrouted end bearing capacity of 1.71 MPa (18 tsf) using Eq. (4) ($N=30$).

Summary and Conclusions

A rational method of predicting the end bearing capacity of post-grouted shafts tipped in cohesionless soils has been developed based on the performance of full scale grouted shaft load tests. The new approach incorporates input parameters such as the service displacement criteria, the attainable grout pressure, and the estimated conventional ungrouted shaft end bearing. Unlike conventional shaft construction and the associated quality assurance methodologies, each and every shaft is tested via the grouting process. Inherently, the grouting then provides quantitative data on the skin friction and end bearing capacity of each shaft. Therefore, grouting verifies a lower limit of total shaft capacity that equals two times the grout pressure acting over the entire tip area. The actual capacity, which is predicted using Eq. (9), is somewhat higher due to an increase in the mobilized end bearing during downward structural loading and the 0.30% increase in side shear from downward instead of upward movement (O'Neill 2002).

As the attainable GPI relies on the side shear capacity on which the grout pressure can react, the aspect ratio (embedment length/diameter) of the drilled shafts should be carefully considered in order to provide the most cost efficient design. Note that potentially stringent lateral loading conditions may govern the foundation design, and may further define the shaft geometry that best supplies the capacities required (both axial and lateral). The methodology presented herein only addresses axial capacity.

The use of grouted shafts has long reaching implications with regards to the state of drilled shaft construction and design. This stems from the unparalleled quality assurance that accompanies the process. Shaft lengths can be reduced and an associated cost savings realized. Further, by statically grout testing each shaft, an increased resistance factor (or lower safety factor) may likely

result for shafts constructed in this fashion. Such an increase in the resistance factor can lead to additional economy.

Acknowledgments

The writers would like to acknowledge the Florida Department of Transportation for funding this study with specific thanks extended to Mr. Peter Lai, the project monitor. Likewise, Auburn University and University of Houston as well as Applied Foundation Testing, Beck Foundation, Coastal Caisson, Driggers Engineering Services, EarthTech, and TreviIcos South are gratefully recognized for their contributions. Therein, Dr. Dan Brown, Dr. Michael O'Neill, Mr. Michael Muchard, Mr. Keith Anderson, Mr. Bud Khouri, Mr. Jaime Driggers, Mr. Ron Broderick, and Mr. Michael Rossie are extended the writers' deepest thanks as well as Rudy, Ltd.

References

- American Association of State Highway and Transportation Officials (AASHTO). (1999). *LRFD bridge design specifications*, SI, 1st Ed., Washington, D.C.
- Bolognesi, A. J. L., and Moretto, O. (1973). "Stage grouting preloading of large piles on sand." *Proc., 8th ICSMFE Cont.*, Moscow.
- Bruce, D. A. (1986). "Enhancing the performance of large diameter piles by grouting." Parts 1 and 2, *Ground Eng.*, ■■■, ■■■-■■■.
- Bruce, D. A., Nufer, P. J., and Triplett, R. E. (1995). "Enhancement of caisson capacity by microfine cement grouting—A recent case history." *Verification of geotechnical grouting*, M. J. Byle and Roy H. Borden, eds., ASCE, New York, 142–152.
- Dapp, S. D. (1998). "Interviews with engineers during load testing on the My Thuan Bridge." Mekong Delta, Vietnam.
- Dapp, S. D. (2002). "Pressure grouting of drilled shafts in sands," PhD dissertation, Univ. of South Florida, Tampa, Fla.
- Dapp, S., and Mullins, G. (2002). "Pressure grouting drilled shaft tips: Full-scale research investigation for silty and shelly sands." *Deep Foundations 2002: An international perspective on theory, design, construction, and performance*, *Geotechnical Special Publication No. 116*, M. W. O'Neill and F. C. Townsend, eds., Vol. 1, ASCE, Reston, Va., 335–350.
- Flemming, W. G. K. (1993). "The improvement of pile performance by base grouting." *Proc., Institution of Civil Engineers*, London.
- Frederick, E. M. (2001). "Pressure grouting drilled shaft tips: Laboratory scale study in a frustum confining vessel." Master's thesis, Univ. of South Florida, Tampa, Fla.
- Gouvenot, D., and Gabiax, F. D. (1975). "A new foundation technique using piles sealed by concrete under high pressure." *Proc., 7th Annual Offshore Technical Conf.*
- Mojabe, M. S., and Duffin, M. J. (1991). "Large diameter, rock socket, base grouted piles in bristol." *Proc., 4th Int. Conf. on Piling and Deep Foundations*, Stresa, Italy.
- Mullins, G. (1999). "Interviews with engineers during load testing on the Taipei Financial Center." Taipei, Taiwan.
- Mullins, G., Dapp, S., Frederick, E., and Wagner, R. (2001). "Pressure grouting drilled shaft tips—Phase I final report." *Final Rep. Submitted Florida Department of Transportation*, Fla.
- Mullins, G., Dapp, S., and Lai, P. (2000). "Pressure-grouting drilled shaft tips in sand." *New technological and design developments in deep foundations*, N. D. Dennis, R. Castelli, and M. W. O'Neill, eds., ASCE, Reston, Va.
- Mullins, G., and O'Neill, M. (2003). "Pressure grouting drilled shaft tips—A full-scale load test program." *Research Rep.*, Univ. of South Florida, Tampa, Fla.

- Mullins, G., and Winters, D. (2004). "Post grouting drilled shaft tips—Phase II final report." *Final Rep. Submitted Florida Department of Transportation*, Fla.
- O'Neill, M. W. (2002). "Discussion of Side resistance in piles and drilled shafts," *J. Geotech. Geoenviron. Eng.*, 127(1), 3–16.
- Piccione, M., Carletti, G., and Diamanti, L. (1984). "The piled foundations of the Al Gazira Hotel in Cairo." *Proc., Int. Conf. on Advances in Piling and Ground Treatment for Foundations*, Institution of Civil Engineers, London.
- Reese, L. C., and O'Neill, M. W. (1988). "Drilled shafts: Construction and design." *FHWA, Publication No. HI-88-042*.
- Santosuossa, M., Rizzi, G., and Diamanti, L. (1991). "Construction of pile foundation of the postal citadel in the direction center of Naples." *Proc. 4th Int. Conf. on Piling and Deep Foundations*, Stresa, Italy.
- Sliwinski, Z. J., and Flemming, W. G. K. (1984). "The integrity and performance of bored piles." *Proc., Int. Conf. on Advances in Piling and Ground Treatment for Foundations*, Institution of Civil Engineers, London.
- Troughton, V. M., and Platis, A. (1989). "The effects of changes in effective stress on a base grouted pile in sand." *Proc. Int. Conf. on Piling and Deep Foundations*, London.